

# Structural and magnetic properties of Fe/ZnSe(001) interfaces

B. Sanyal<sup>†1</sup> and S. Mirbt<sup>2</sup>

*Department of Physics, Uppsala University, Uppsala, Sweden*

<sup>†</sup> *present address : Maxlab, Lund University, Sweden*

## Abstract

We have performed first principles electronic structure calculations to investigate the structural and magnetic properties of Fe/ZnSe(001) interfaces. Calculations involving full geometry optimizations have been carried out for a broad range of thickness of Fe layers(0.5 monolayer to 10 monolayers) on top of a ZnSe(001) substrate. Both Zn and Se terminated interfaces have been explored. Total energy calculations show that Se segregates at the surface which is in agreement with recent experiments. For both Zn and Se terminations, the interface Fe magnetic moments are higher than the bulk bcc Fe moment. We have also investigated the effect of adding Fe atoms on top of a reconstructed ZnSe surface to explore the role of reconstruction of semiconductor surfaces in determining properties of metal-semiconductor interfaces. Fe breaks the Se dimer bond formed for a Se-rich (2x1) reconstructed surface. Finally, we looked at the reverse growth i.e. growth of Zn and Se atoms on a bcc Fe(001) substrate to investigate the properties of the second interface of a magnetotunnel junction. The results are in good agreement with the theoretical and experimental results, wherever available.

PACS numbers: 75.70.-i,73.20.At,73.40.Sx

Typeset using REVTeX

## I. INTRODUCTION

Spin electronics is one of the major topics of research nowadays where one combines the charge and spin degrees of freedom of carriers<sup>1</sup>. This has got immense applications in modern technology e.g. magnetic recording industry and semiconductor appliances. The recent exciting suggestions are to fabricate spin transistors and spin polarized tunneling junctions made up of ferromagnetic metals and semiconductors. Large tunneling magnetoresistance (TMR) has been observed experimentally for heterostructures built of dilute magnetic semiconductors (DMS). There are also theoretical predictions of large TMR for heterostructures based on Fe and semiconductors<sup>2</sup>. In this context, the interface between a metal and a semiconductor plays a crucial role in determining the magnetic and hence the transport properties of the hybrid systems as the injection of a spin-polarized electron from a magnetic material to the semiconductor depends crucially on the interface properties. The typical semiconductors used for these purposes are GaAs and ZnSe which belong to III-V and II-VI compounds respectively. In such devices Fe is one of the most commonly used 3d metal as it has got a high Curie temperature.

Informations about the structural and magnetic properties of the interface between Fe and ZnSe are available from experiments<sup>3-5</sup>. Jonker *et al.* studied Fe growth on ZnSe(001) at 450 K. The growth was smooth and epitaxial. However, they observed a reduction in magnetic moment of Fe compared to the bulk value. Recently, Reiger *et al.*<sup>5</sup> studied Fe growth on ZnSe(001) at room temperature and found a three dimensional nucleation at the beginning of the growth process followed by a coalescence of the 3D islands around 7 monolayers(ML). There was no reduction of the Fe magnetic moment even for a low Fe coverage.

Theoretical investigations by ab-initio electronic structure calculations have been done for Fe/ZnSe interfaces and multilayers<sup>2,7,8,9</sup>. Continenza *et al.*<sup>7</sup> studied various Fe/ZnSe superlattices by all-electron full potential linearized augmented plane wave method within the local spin density approximation. They concluded that the enhanced Fe magnetism is

suppressed as the Fe thickness is increased and the interface effects rapidly die out in the inner Fe layers. de Jonge *et al.*<sup>8</sup> have performed first principles electronic structure calculations of superlattices of Fe and several semiconductors (Ge, GaAs and ZnSe) by a localized spherical wave method. Butler *et al.*<sup>2</sup> studied the tunneling structures of ferromagnets and semiconductors by a layer Korringa-Kohn-Rostoker (LKKR) method. Moreover, they have investigated<sup>10</sup> extensively the transport properties of magnetotunnel junctions of Fe and ZnSe using Landauer approach for the calculation of conductance.

All the above theoretical calculations were done for ideal interfaces i.e. the metal and semiconductor atoms followed a regular stacking. In this paper, we study the relaxed Fe/ZnSe interface, i.e we allow for ionic, shape, and volume relaxations. We do not consider any temperature driven reconstruction except segregation, because it is known, that the semiconductor constituents segregate<sup>11</sup> towards the surface when they are in contact with a metal. (We compared the total energies of different atomic configurations to investigate the surface segregation of Zn and Se.) We study (section III) the dependence of the interface electronic properties on the Fe film thickness and the semiconductor termination. Since, for a magnetotunnel structure, two interfaces are formed between Fe and ZnSe, we also studied (section IV) the reverse growth i.e. Zn or Se on a bcc Fe(001) substrate. Moreover, we investigate (section V) the importance of the semiconductor surface reconstruction for the interface formation.

## II. COMPUTATIONAL DETAILS

Calculations have been performed by a self-consistent first-principles plane wave pseudopotential code (VASP)<sup>15</sup>. Vanderbilt type ultrasoft pseudopotentials<sup>14</sup> were used for the calculations which are reported to work well for transition metals<sup>16</sup>. More accurate PAW (projector augmented wave)<sup>17</sup> pseudopotentials were also used in some cases for testing of accuracy. Calculations reveal that the ultrasoft pseudopotentials are good enough to reproduce results with reasonable accuracies. An energy cut-off of 250 eV was used for the

kinetic energy of plane waves in the basis set. We have checked thoroughly that this cut-off energy is sufficient as it produces negligible Pulay stress. Perdew-Wang GGA (generalized gradient approximation) exchange -correlation<sup>18</sup> was used instead of LSDA (local spin density approximation). LSDA description of the Fe ground state structure is inappropriate and the structural informations of Fe layers obtained from geometry optimizations might be incorrect. We used a (1x1) unreconstructed surface cell with at least 10 Å vacuum and six monolayers of ZnSe (three Zn and three Se layers). The number of Fe atoms varied from 1 (0.5 ML) to 20 (10 MLs) in the unit cell. The bulk layer at the bottom was terminated with two pseudo hydrogen atoms to avoid charge sloshing<sup>19</sup>. Two layers of ZnSe (one Zn and one Se) together with the pseudo hydrogen atoms were kept unrelaxed at the ideal bulk positions. It is to be noted that the lattice constant of bcc Fe is almost half of that of ZnSe. This helps Fe to grow in a bcc phase on a ZnSe(001) substrate without appreciable strain. Our calculations with GGA yield equilibrium lattice constants of bcc Fe and zinc-blende ZnSe systems to be 2.86 Å and 5.75 Å respectively. The experimental lattice constant of ZnSe is 5.66 Å and the overestimation of the calculated one is obvious for using GGA. Thus in experiment the Fe lattice constant is 1.4 % smaller than the ZnSe lattice constant, whereas in our calculation the Fe lattice constant is 0.5 % larger. The calculated direct band gap at the  $\Gamma$  point for the equilibrium lattice parameter is small (1.14 eV) compared to the experimental band gap (2.8 eV). As a first step, we didn't attempt to correct that but this correction might be important from the point of view of metal-semiconductor junction properties. Total energies were always converged upto  $10^{-4}$  eV for electronic relaxations and  $10^{-3}$  eV for ionic relaxations. The atomic positions were relaxed alongwith the volume and shape of the unit cells. The full optimization with relaxations of internal and external degrees of freedom is important as far as magnetism is concerned. Forces were converged with a tolerance of  $10^{-2}$  eV/Å . The Monkhorst-Pack scheme<sup>20</sup> was used for the generation of special k-points in the Brillouin zone. Convergence was checked carefully with respect to the number of k-points used. For example, a  $6 \times 6 \times 2$  mesh for k points was used for the largest unit cell containing 20 Fe atoms which yielded 36 k points in the irreducible Brillouin

zone (IBZ) for the accurate calculation of DOS by tetrahedron method. For smaller cells, we used 108 k points in IBZ. For the relaxation of the atoms, smaller set of k-points were used (5 k-points in IBZ for a 20 atom cell) alongwith the Gaussian smearing of k-points. It should be mentioned here that there is no unambiguous way of determining the local properties e.g. local density of states, local magnetic moments etc. for a plane-wave method as the radius within which these properties are sought is not well defined. The plane wave components of the eigenstates were projected on linear combinations of spherical waves inside the atomic spheres around the atoms. The coefficients of the local spherical waves were used to construct the angular momentum projected local DOS. Details have been discussed by Eichler *et al.*<sup>21</sup>. For the present calculations, the radii of Fe, Zn and Se atoms were chosen to be 1.41 Å 1.35 Å and 1.48 Å respectively. These values were taken from the calculations of bulk bcc Fe and bulk ZnSe systems.

### III. DIFFERENT FE COVERAGES

#### A. 0.5 ML coverage

We first present results for the calculations involving ideal stacking positions. Though this situation is not energetically favourable compared to the relaxed case, we investigate this as a starting point. Total energies are compared for the two cases (i) Fe is on the top of the ZnSe substrate in a regular stacking position (ii) Fe is in a substitutional Zn (Se) site in a subsurface layer in exchange with a Zn (Se) atom kept on the surface. We have found that Fe in a substitutional Zn site in the subsurface layer is more favourable than Fe being on the surface. The energy difference between the two configurations is 0.83 eV/cell. But, for Se substitution, Fe prefers to sit in the surface keeping the Se atom in the subsurface layer. Here, the energy difference is 0.40 eV/cell. However, these cases without relaxations are unfavourable compared to the relaxed case. It is well known that in the case of dilute magnetic semiconductors (DMS) of (Fe,Zn)Se<sup>22</sup>, Fe prefers to sit in the cation site. For this

case, the calculated Fe-Se distance (2.47 Å) is slightly smaller than the Zn-Se bondlength (2.49 Å), whereas the measured Fe-Se distance (2.48 Å) is slightly larger than the measured Zn-Se bondlength (2.45 Å). The magnetism is atomic like with an integer magnetic moment of  $4.00 \mu_B/\text{cell}$ .

Now we discuss the results of the relaxation studies. The structure of the region very close to the interface of a metal and a semiconductor is an important factor for spin injection from a metal to a semiconductor. Since semiconductors have open structures, the metal atom will proceed inside the semiconducting substrate, where the charge overlap with the substrate atoms is increased. To investigate this possibility, an approximate energy landscape has been calculated by putting half a monolayer of Fe in different positions on and inside the host ZnSe lattice and comparing the total energies. The result is shown in Fig.1 for a Se-terminated surface. The energy difference is defined as  $\Delta E = E_{tot}^B - E_{tot}^S$  where  $E_{tot}^S$  is the total energy for an Fe atom sitting in the regular position on top of the surface and  $E_{tot}^B$  is the total energy of the Fe atom sitting on different positions within the substrate. The most preferable position we found to be an interstitial one which is 2.875 Å below the surface. The corresponding total magnetic moments of the unit cells are plotted in the inset.

The final atomic configurations of the most preferable positions are shown in Fig. 2(a-c) and 3(a-c) for the Zn and Se terminated cases respectively. One can note the difference in the relaxations in the two cases: For a Zn-terminated case (shown in Fig. 2), with relaxations of atoms, the surface Zn atom moves upwards leaving a vacancy which is eventually occupied by the buried Fe. The topmost Zn atom occupies an ideal stacking position. This also conforms with the unrelaxed calculation mentioned above.

For a Se terminated case (shown in Fig. 3), starting from an identical situation as before, Se moves a little bit upwards. The buried Fe atom remains more or less in the interstitial position. So, the distinct difference in the two cases is the site occupancy of Fe. In both cases, relaxation leads to lower total energies compared to the cases of unrelaxed regular stacking as discussed before (0.03 eV/cell and 0.8 eV/cell lower for Zn and Se terminated

cases respectively). It is seen that for Zn termination, the nearest Fe-Zn and Fe-Se distances are 2.49 Å and 2.37 Å respectively. For Se coverage, the distances are 2.96 Å and 2.52 Å respectively.

(So, magnetic moment is enhanced compared to that of bulk bcc Fe. However, it should be kept in mind that as we are using GGA, calculated value of magnetic moment ( $2.33 \mu_B$ ) is greater than the experimental value of  $2.2 \mu_B$  for bulk bcc Fe.)

Atom and orbital projected DOSs are shown in Fig. 2(d-h) and Fig. 3(d-h) for Zn and Se terminated cases respectively. For both terminations, the majority Fe DOS has no states at the Fermi energy and we find an atomic like integer moment of  $3.00 \mu_B$  for the unit cell. This is not found for cases without relaxations described before. The magnetic moments for the unrelaxed cases are greater and of non-integer type. Half metallicity is seen only when relaxation is allowed. Half metallic systems (a system where one finds a metallic DOS for one spin channel and semiconducting DOS for the other showing 100 % spin polarization at the Fermi energy) are extremely important in the context of magnetoelectronics involving spin transport between ferromagnetic systems across a semiconducting/insulating barrier. However, with increased Fe coverage, this behavior dies out and we arrive at a normal metallic DOS. A similar calculation for Co for 0.5 ML coverage also yields an integer moment of  $2.00 \mu_B/\text{cell}$  with both Zn and Se on top of buried Co.

Comparing this case with the total magnetic moment of  $4.00 \mu_B$  of a bulk DMS (Fe,Zn)Se, it is clear that the difference is due to the occupancy of the minority spin states of Fe as the majority states are completely occupied for the two cases. In DMSs, Hund's rule for the atomic moment is followed resulting in the occupation of 5 and 1 electrons in the majority and minority spin channels of Fe *d*-states respectively. In the present case, again Hund's rule for the atomic moment is followed, but Fe has gained one electron, such that now two electrons are in the minority spin channel. The reason is the following: At the ideal surface, i.e without Fe, the two Zn (Se) dangling bonds (DB) are each partially occupied with 0.5 (1.5) electrons. A semiconductor gains energy by having either occupied or unoccupied DB. Usually, anion DB (Se) are fully occupied and cation (Zn) DB are empty. Therefore, taking



one electron from the Zn (Se) DB will lead to either occupied or unoccupied DB: for the Zn termination two empty DB and for the Se termination one empty and one occupied DB. This electron from the DB is transferred to Fe and gives rise to the two electrons in the d-minority channel.

Now, let us look at the projected DOS in detail. In both sets of figures (fig. 2(d-h) and fig. 3(d-h)), Fe *s* and *d* states, Zn *s*, *p* and *d* states and Se *s* and *p* states are shown (see figure captions for details). The energy scale is chosen to avoid showing the huge peak for Zn 3*d* state which is deep in energy and doesn't hybridize with the Fe *d* states. For both terminations, the Fe DOS looks quite different from that of bcc bulk Fe. The majority spin states are filled up for Fe. For Zn termination, in Figs. 2(e) and 2(g), projected DOSs for surface(Zn<sub>1</sub>) and sub-surface Zn(Zn<sub>2</sub>) atoms are shown. The relative distribution of *s* and *p* states are different with the subsurface Zn (Fig.2(g)) having more bulk like character. Fe *d* states are narrower compared to the same for Se-terminated case (see Fig. 3(d)) due to less number of nearest neighbours in a substitutional position compared to an interstitial position for Se terminated case. This yields a slightly larger local magnetic moment of Fe for the Se terminated case (Table I). For Se termination, the effect of the Fe atom sitting in an interstitial position is pronounced even in the states of the atoms of deep subsurface layers e.g. Se<sub>2</sub> and Zn<sub>2</sub>. The sharp peaks in the conduction bands have mostly Zn 4*s* and Se 4*s* and 4*p* characters. The induced spin polarizations of Zn and Se atoms at the surface are evident from the relative shift of majority and minority states (Table I).

### B. 1.5 ML coverage

This case corresponds to 3 Fe atoms in the unit cell. As a complete Fe monolayer should contain 2 Fe atoms and already 1 Fe atom is burried in a subsurface layer, it is interesting to find the configuration with the segregated Se atom. For a Se terminated cases, we explored three different situations to find the lowest energy configuration (see Fig. 4). In Fig. 4(a), Se is sitting at a subsurface layer covered by a complete Fe layer at the surface. In Fig.

4(b), the surface is covered by 0.5 ML of Fe and Se is still in a subsurface layer. Finally, in Fig. 4(c), Se is at the surface followed by a complete Fe monolayer. The resulting sequence of energetics is  $E_c < E_b < E_a$ . The energy difference between configuration (c) and (b) is quite large (2.6 eV/cell). So, in summary, Se segregates towards the surface. In all cases, the magnetism is almost similar. In the most favourable case (c), the two Fe atoms (indexed 1 and 2 in the figure) below the surface have magnetic moments of  $2.84 \mu_B$  and  $2.66 \mu_B$  respectively. The buried Fe atom (indexed as 3) has a magnetic moment of  $2.92 \mu_B$ . The surface Se atom (indexed as 4) attains an induced magnetic moment of  $0.07 \mu_B$ . Fe(1)-Se(4) distance is  $2.48 \text{ \AA}$  which is different than the cases where Fe and Se lie almost in the same layer. Though we have performed calculations for different thicknesses of Fe layers, we present only the details of the important ones. The next section describes a case with a relatively thick Fe layer.

### C. 20 atoms (10 MLs) of Fe

To see the effect of the interface on the bulk Fe atom like layers, we performed calculations with 20 atoms of Fe on ZnSe substrate. We explored both the cases of Se-segregated and non segregated cases. The configuration with Se at the surface has the lower energy (energy difference between the surface segregated and non-segregated profiles is 1.5 eV/cell). For a Se-segregated case, the surface Fe-Se distance is  $2.81 \text{ \AA}$ . Magnetic moment of the surface Fe atom is  $2.96 \mu_B$ . The buried Fe atom in the interface has a moment of  $2.88 \mu_B$  with a Fe-Zn distance of  $2.87 \text{ \AA}$ . Informations about the structural and magnetic properties are listed in table II for a few selected cases.

In Fig. 5, we have shown the layer projected local magnetic moments for the case of 20 Fe atoms deposited on ZnSe. The surface and the interface Fe atoms have large magnetic moments compared to the bulk value. But the atoms attain the magnetic moments of bulk bcc Fe very near to the interface. The induced moments on Se and Zn atoms close to Fe are parallel and antiparallel with respect to Fe moments. The corresponding projected DOSs

are shown in Fig. 6. Figs. 6(a) and 6(b) show the surface Fe and Se atoms respectively. Fig. 6(c) shows the PDOS for an Fe atom in an intermediate Fe monolayer and (d) shows the same approaching the interface. Figs. 6(e) and (f) are PDOSs of buried interface Fe atom and Zn atom respectively. For the surface atom, the majority DOS is full whereas the minority DOS is partly occupied. Both the bonding and the antibonding  $d$  states of majority spin are filled whereas the bonding states for minority spin are occupied leaving the antibonding state fully empty. Fig. 6(c) corresponds to the bulk bcc Fe DOS where the majority states are occupied (both bonding and the antibonding states are filled) and the Fermi level lies at the pseudogap of the minority DOS separating bonding and antibonding  $d$  states. The majority DOS is more affected than the minority one while going from surface to the interface. Approaching the interface, the exchange splitting between the majority and minority DOSs increase and for the interface atom which is marked as  $\text{Fe}_I$ , the minority DOS is pushed towards the low energy side. DOS looks similar to that obtained by other authors<sup>8</sup>. DOS at Fermi level is considerably different for different Fe atoms. The spin polarization SP is defined as  $\text{SP} = \frac{n(E_F)_\uparrow - n(E_F)_\downarrow}{n(E_F)_\uparrow + n(E_F)_\downarrow}$  where  $n(E_F)_\sigma$  is the DOS at Fermi level for spin  $\sigma = \uparrow, \downarrow$ . SP is different for different Fe atoms. It is increased for the surface and the interface Fe atoms (negative) whereas it has got a lower value (positive) for the bulk like Fe atom.

In Fig. 7, we show the total and averaged magnetic moments of Fe atoms per unit cell as a function of Fe thickness. The values of the total magnetic moment increases linearly with Fe thickness. This is also seen in experiments<sup>5</sup>. The value of the slope is close to the bulk Fe moment but still larger because of the presence of Fe surface atoms. For Fe/GaAs(001) interface, it is seen from experiments<sup>6</sup> that the extrapolated curve in a magnetic moment vs. thickness plot touches the thickness axis above the zero value. This means that for low thickness, magnetism of the interface is reduced compared to the bulk value. The same for Fe/ZnSe(001) interface doesn't show any reduction of magnetic moment at the interface. The reason is that the p-d wavefunction overlap between Fe and As is stronger than between Fe and Se. For example, the Fe magnetic moment in an As environment is

considerably reduced, whereas it is atomic like in a Se environment. The inset shows the averaged magnetic moment per Fe atom in the cell as a function of Fe thickness. Averaged moment is defined as the ratio of the total magnetic moment and the number of Fe atoms in the unit cell. It is seen that this value decreases with thicker Fe layer and approaches the bulk magnetic moment of Fe. This is understandable because as we deposit more and more Fe atoms, the effect of surface and interface washes out and the bulk character is achieved.

The DOSs at the Fermi levels for both Se and Zn terminated cases are depicted in Fig. 8. It is to be noted that for these cases, surface segregation of Se and Zn atoms have also been considered. For that reason, a Zn atom is close to Fe for a Se-terminated case and a Se atom is close to Fe for a Zn-terminated case. A segregated profile for a Zn-terminated case has been chosen intentionally to have a comparative study with the Se-terminated case though Zn segregation has not been confirmed by the experiments. The sequence of the atoms from left to right is from the interface towards the bulk semiconductor. For 1 Fe atom, the spin polarization(SP) is -1.0(i.e. 100 % spin polarization). For 4 and 20 Fe atoms, the spin polarization is reduced. For the thickest layer i.e. 20 atoms of Fe, we find that the spin polarization reduces faster to zero as one approaches the bulk layers. For Se terminated cases (figs. 8(a-c)), spin polarization is always negative but for Zn terminated cases, the same for 4 and 20 atoms Fe (figs. 8(e-f)) shows positive values.

#### IV. REVERSE GROWTH

To prepare a magnetotunnel junction, one has to care for two interfaces. One where the semiconductor atoms are deposited on the metal electrode and the other where the metal electrode atoms are deposited on semiconductor substrate. It has been observed by transmission electron microscopy<sup>23</sup> that the interface structures are not the same for the two cases. The upper interface (Fe/ZnSe) is rougher than the lower one (ZnSe/Fe). To investigate this, we have done very simple calculations where we put either Zn or Se atoms on a bcc Fe(001) substrate. We compared the total energies of two configurations (i) Zn or

Se atom is on top of Fe substrate (ii) Zn or Se atom is in a subsurface layer covered by one Fe layer at top. We have found that the semiconductor constituents prefer to sit on top of a Fe substrate indicating a sharp interface. For Se, the energy difference is 2.15 eV/cell whereas for Zn, it is 0.9 eV/cell. It suggests that Se/Fe interface is less probable to be a mixed one compared to the Zn/Fe interface. However, the magnetic moments are not changed appreciably for different configurations. We have already reported in the previous sections that for Fe/ZnSe interface, half a monolayer of Fe prefers to stay in a buried position in the ZnSe host. We can conclude that this interface is less sharp than the one with the reverse growth.

## V. FE ON A RECONSTRUCTED SURFACE

In this section, we present the results of depositing Fe atoms on a Se-rich (2x1) reconstructed surface. It is already known from experiments<sup>12</sup> and theoretical calculations<sup>13</sup> that the Zn-rich and Se-rich surfaces undergo c(2x2) and (2x1) surface reconstructions respectively. For a Se-rich (2x1) reconstructed surface, a Se dimer of bond-length 2.40 Å is formed on the surface<sup>13</sup>. We have put 2 Fe atoms on top of a Se-rich (2x1) reconstructed surface having a Se dimer (Se1 and Se2) and started relaxing the atoms. In the final relaxed configuration, 1 Fe atom sits in the same layer as one of the Se atoms(Se1) of the dimer breaking the Se dimer bond. The distance between Se1 and Se2 atoms becomes 5.24 Å. As the Se dimer is broken, the effect of the reconstructed semiconductor substrate is diminished. The other Se atom(Se2) goes beneath the layer. Another Fe atom goes to the surface. This is in accordance with all the cases where 1 Fe atom wants to be buried under the Zn or Se layer. The bond length between two Fe atoms and Se1 is 2.50 Å each. The magnetic moment is increased compared to the unreconstructed case by 0.5  $\mu_B$ /cell. This increase is due to the lack of nearest neighbours of the topmost Fe atom. As the signature of the reconstructed semiconductor substrate is lost, we therefore conclude that the surface reconstruction has no dramatic effect in determining the properties of the Fe-ZnSe interfaces.

## VI. CONCLUSION

In this paper, we have extensively studied structural and magnetic properties of Fe/ZnSe(001) interfaces. Geometry optimizations have provided useful structural informations of the interface. Our results show that half a monolayer of Fe prefers to sit below the surface. For the Se terminated case, Fe prefers to sit in the interstitial site whereas for Zn terminated case, Fe prefers a Zn substitutional site. We have observed surface segregation of Zn and Se atoms. However, the magnetic properties are not changed appreciably for segregated and non-segregated profiles. Magnetic moment of the interface Fe atom is increased compared to the bulk bcc Fe moment for both Zn and Se terminations. Fe attains its bulk moment very close to the interface. A reverse growth i.e. Zn or Se on top of the bcc Fe surface has also been studied. For a Se-rich (2x1) reconstructed surface, Fe breaks the Se dimer bond and sits in between to have a proper bonding configuration. Effect of the reconstructed semiconductor substrate is diminished.

## ACKNOWLEDGMENTS

S.M. is grateful to the Swedish Natural Science Research Council and Göran Gustafsson Foundation for financial support.

## REFERENCES

- <sup>1</sup> email :Biplab.Sanyal@maxlab.lu.se
- <sup>2</sup> email :susanne@fysik.uu.se
- <sup>1</sup> G. A. Prinz, Phys. today **48**, 58 (1995); Science **282**, 1660 (1998).
- <sup>2</sup> W. H. Butler, X.-G. Zhang, X.-D. Wang, J. van Ek and J. M. Maclaren, J. Appl. Phys. **81**, 5518 (1997).
- <sup>3</sup> J. J. Krebs, B. T. Jonker and G. A. Prinz, J. Appl. Phys. **61**, 3744 (1987).
- <sup>4</sup> B. T. Jonker, G. A. Prinz and Y. U. Idzerda, J. Vac. Sc. Technol. B **9**, 2437 (1991).
- <sup>5</sup> E. Reiger, E. Reinwald, G. Garreau, M. Ernst, M. Zolff, F. Bensch, S. Bauer, H. Preis and G. Bayreuther, J. Appl. Phys. **87**, 5923 (2000).
- <sup>6</sup> A. Filipe, A. Schuhl and P. Galtier, Appl. Phys. Lett. **70**, 129 (1997); A. Filipe and A. Schuhl, J. Appl. Phys. **81**, 4359 (1997).
- <sup>7</sup> A. Continenza, S. Massidda and A. J. Freeman, Phys. Rev. B **42**, 2904 (1990).
- <sup>8</sup> D. de Jonge, P. K. de Boer and R. A. de Groot, Phys. Rev. B **60**, 5529 (1999).
- <sup>9</sup> Ph. Mavropoulos, N. Papanikolaou and P. H. Dederichs, Phys. Rev. Lett. **85**, 1088 (2000).
- <sup>10</sup> J. M. Maclaren, X.-G. Zhang, W. H. Butler and X.-D. Wang, Phys. Rev. B **59**, 5470 (1999).
- <sup>11</sup> J. H. Weaver, Z. lin and F. Xu, in *Surface segregation phenomena*, ed. by P. A. Dowben and A. Miller, CRC Press Inc., p. 259 (1990).
- <sup>12</sup> A. Ohtake, T. Hanada, T. Yasuda, K. Arai and T. Yao, Phys. Rev. B **60**, 8326 (1999).
- <sup>13</sup> C. H. Park and D. J. Chadi, Phys. Rev. B **49**, 16467 (1994).
- <sup>14</sup> D. Vanderbilt, Phys. Rev. B **41**, 7892 (1990).

- <sup>15</sup> G. Kresse and J. Hafner, Phys. Rev. B **47**, RC558 (1993); G. Kresse and J. Furthmüller, Phys. Rev. B **54**, 11169 (1996).
- <sup>16</sup> E. G. Moroni, G. Kresse, J. Hafner and J. Furthmüller, Phys. Rev. B **56**, 15629 (1997).
- <sup>17</sup> P.E. Blöchel, Phys. Rev. B **50**, 17953 (1994).
- <sup>18</sup> J. P. Perdew and Y. Yang, Phys. Rev. B **45**, 13244 (1992).
- <sup>19</sup> N. Moll, A. Kley, E. Pehlke and M. Scheffler, Phys. Rev. B **54**, 8844 (1996).
- <sup>20</sup> H. J. Monkhorst and J. D. Pack, Phys. Rev. B **13**, 5188 (1976).
- <sup>21</sup> A. Eichler, J. Hafner, J. Furthmüller and G. Kresse, Surface Science **346**, 300 (1996).
- <sup>22</sup> W. J. M. de Jonge and H. J. M. Swagten, J. Mag. Magn. Mat. **100**, 322 (1991).
- <sup>23</sup> F. Gustavsson, *Licenciate thesis*, Uppsala University (2000).



## FIGURES

FIG. 1. Energy difference plotted as a function of the distance (in Å) of the Fe atom from the Se-terminated surface. See text for the details.

FIG. 2. Final relaxed configuration (a-c) from different perspectives and corresponding atom and orbital projected DOSs for 0.5 ML Fe on a Zn-terminated surface. For figures (a-c), open circles, filled circles and open squares denote Zn, Fe and Se atoms respectively. Vac. represents vacuum and the two vertical dashed lines denote the basic (1x1) unit cell. Lines are drawn between atoms to show the bonds of the host zinc-blende lattice. For figures (d-h), besides Fe, Zn and Se atoms are indexed according to the stacking in unit cell from surface towards the bulk. Appropriate legends are provided for the orbitals in the figures. The vertical lines in figures (d-h) represent the Fermi level.

FIG. 3. Same as Fig. 1 but for a Se-terminated case.

FIG. 4. Final relaxed configurations for 1.5 ML of Fe (3 Fe atoms in the unit cell) on a Se-terminated surface. (a) A complete ML of Fe at the surface and Se is at the interface (b) Se has gone towards the surface (c) Se covers the surface followed by Fe atoms. The other notations are similar to those of Fig.1 and Fig.2.

FIG. 5. Layer projected magnetic moments for the case of 20 Fe atoms on Se-terminated (and segregated) surface. Note that for each Fe monolayer, there are two Fe atoms except for the surface and interface. The bold line indicates the zero value and the dashed line indicates the calculated magnetic moment for bcc bulk Fe within GGA.

FIG. 6. Selected atom and orbital projected spin-resolved DOS for the case described in the previous figure. The sequence of the figures is (a) surface Fe atom ( $Fe_S$ )(b) segregated Se atom ( $Se_S$ )(c) Fe at some intermediate layer ( $Fe_B$ ) (d) Fe approaching the interface( $Fe_{B-I}$ ) (e) Fe at the interface( $Fe_I$ ) (f) Zn close to Fe at the interface( $Zn_I$ ). The vertical lines show the position of the Fermi energy.

FIG. 7. Evolution of magnetic moment with increasing number of Fe atoms in the unit cell. The graph is for Se terminated and segregated case. The bold line is the fitted one with the calculated data (dashed line). (Inset) Average Fe moment/unit cell vs. number of Fe atoms.

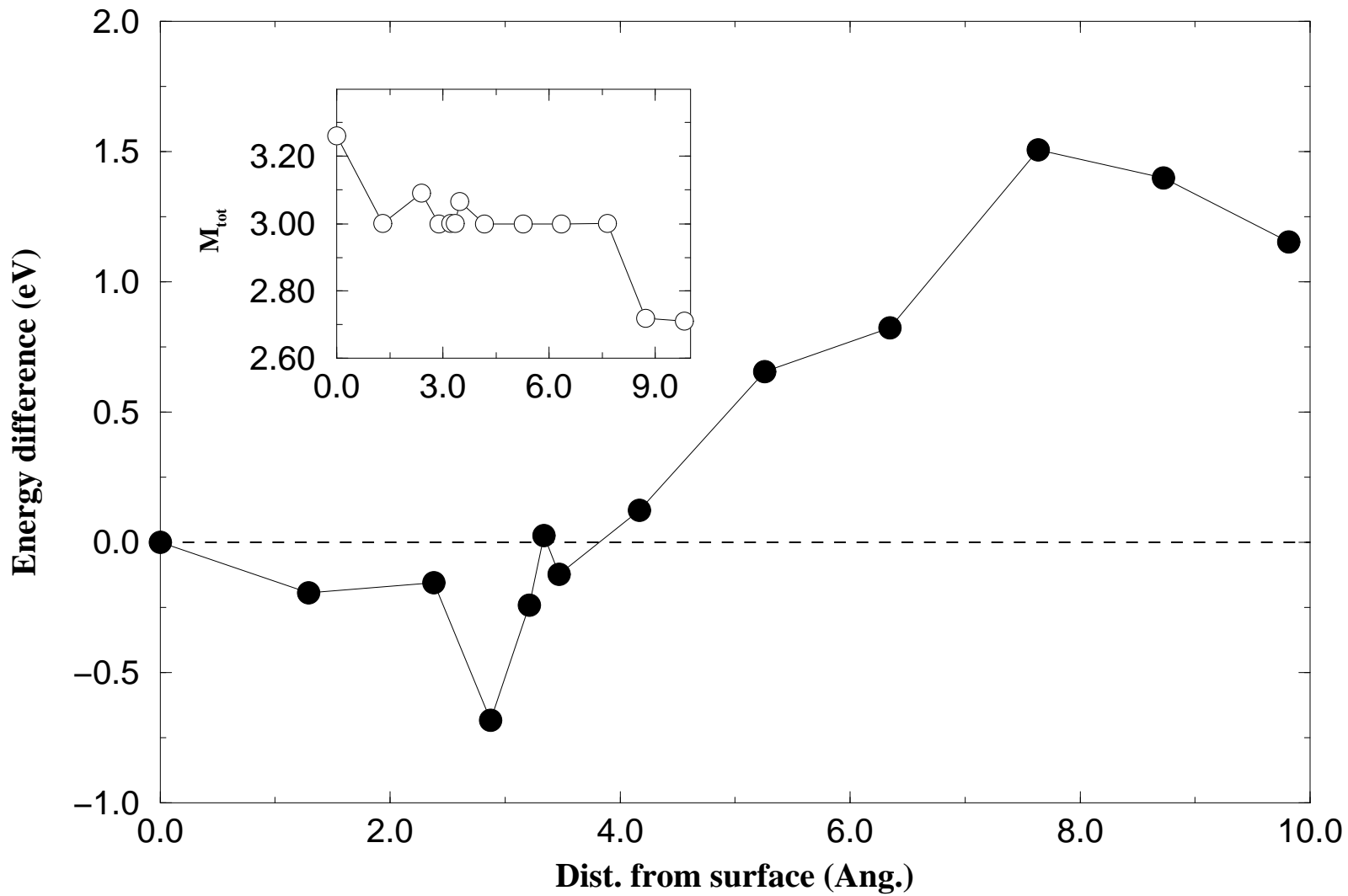
FIG. 8. Densities of states at Fermi level  $n(E_F)$  for (left) Se terminated and segregated and (right) Zn terminated and segregated cases. (a) and (d) are for 1 Fe atom, (b) and (e) are for 4 Fe atoms and (c) and (f) are for 20 Fe atoms. The upper triangle plots are for the majority spin electrons whereas the lower triangles are for the minority spin electrons. The sequence of the atoms is from the interface towards the bulk semiconductor (left to the right of the figures).

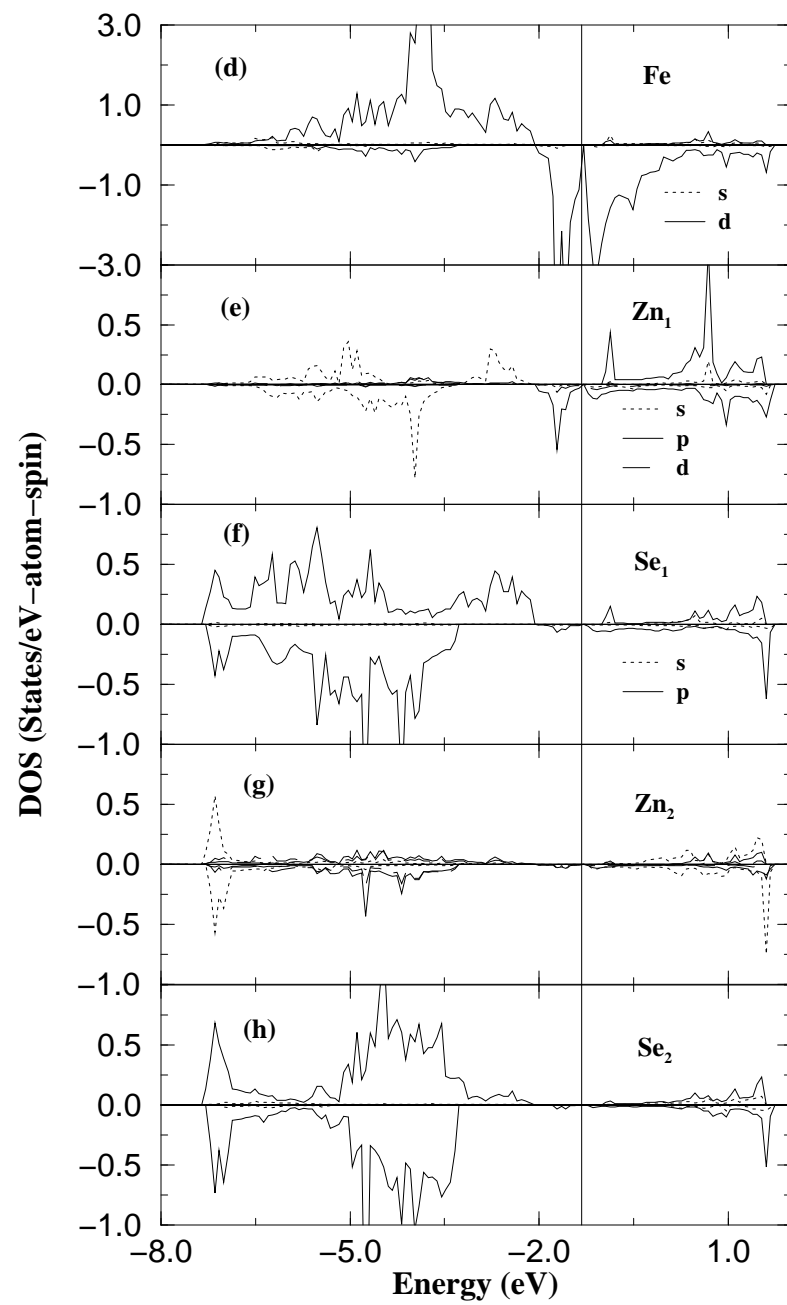
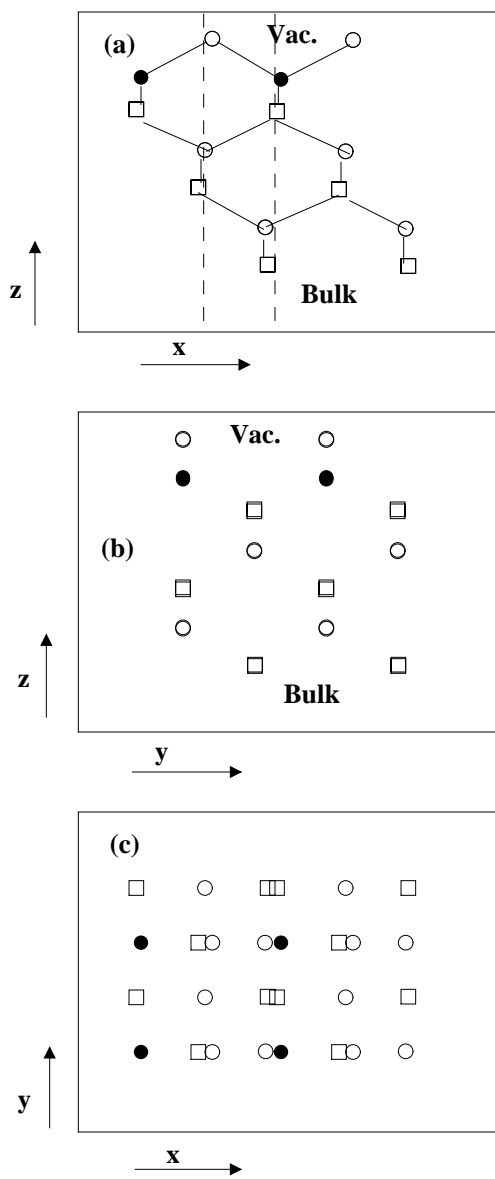
**TABLE I.** Magnetic moments (in  $\mu_B$ ) for 0.5 ML of Fe.

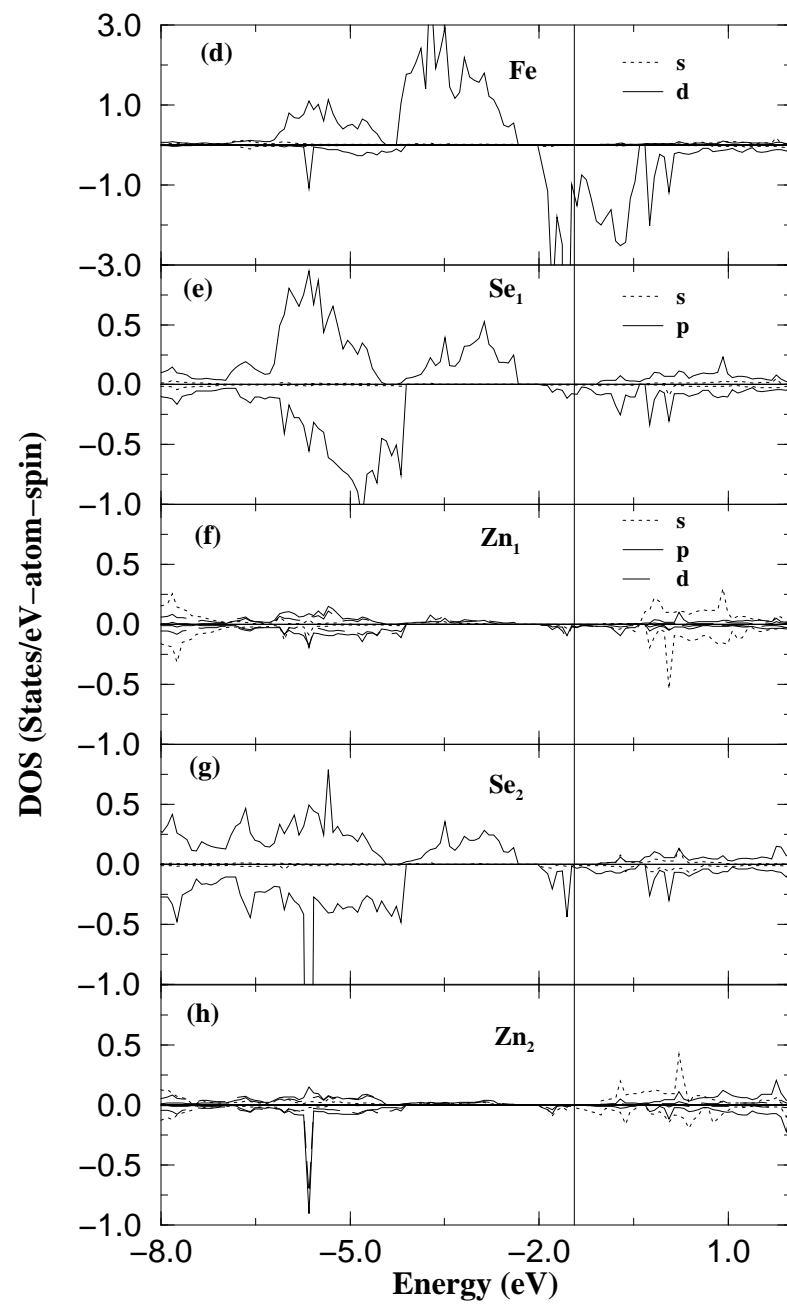
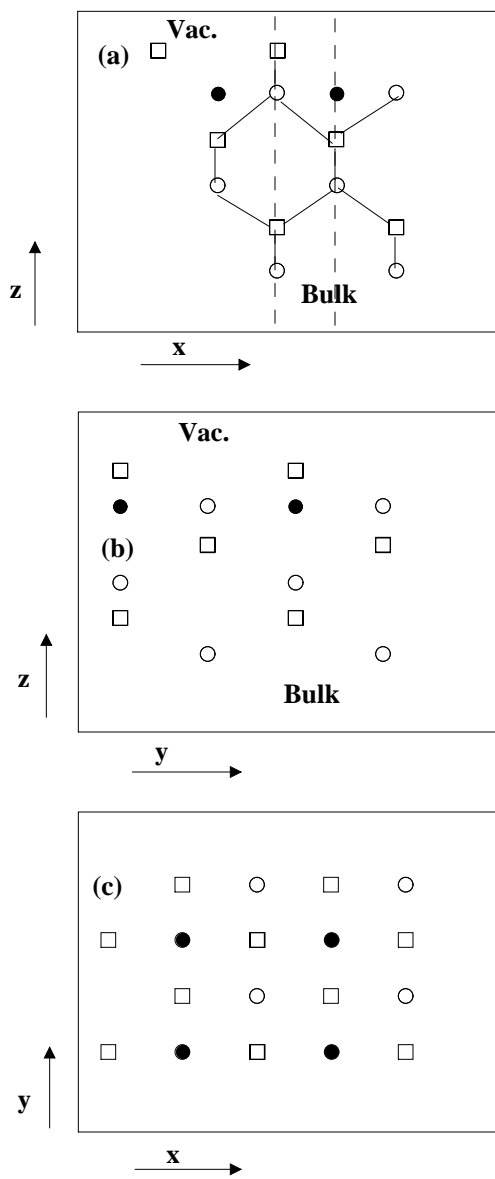
	Fe moment	surface Zn moment	surface Se moment	total moment/cell
Zn-terminated	2.93	-0.023		3.00
Se-terminated	2.84		0.08	3.00

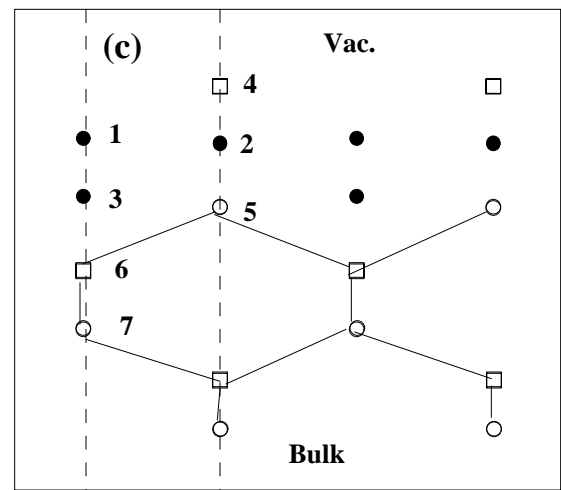
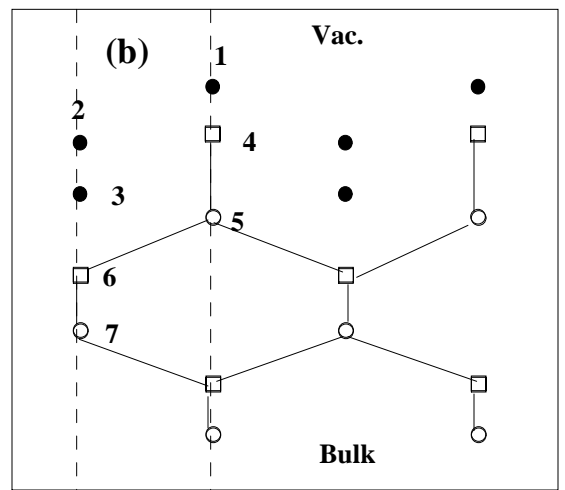
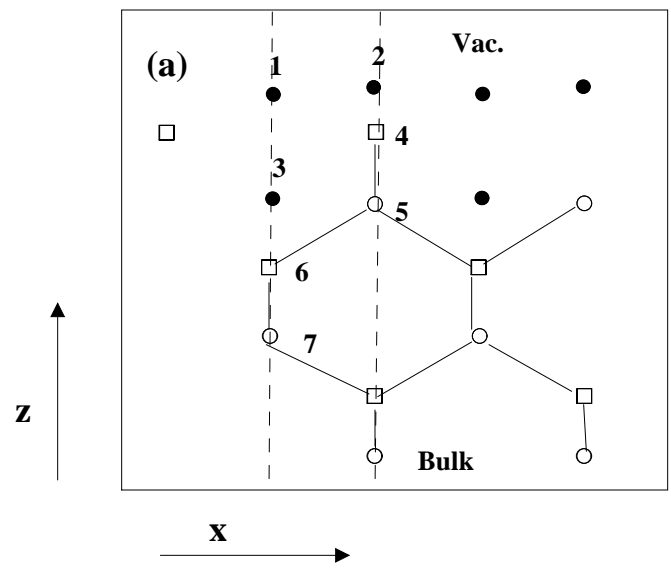
**TABLE II.** Structural and magnetic informations for selected thicknesses of Fe layers. All these results are for Se-terminated and segregated cases. The subscripts  $S$  and  $I$  denote surface and interface atoms.  $\text{Fe}_I$  is in the burried position close to the interface Zn atom. The values in the parentheses  $()^\dagger$  and  $()^*$  are for  $\text{Fe}_S\text{-Zn}_S$  and  $\text{Fe}_I\text{-Se}_I$  distances for a Zn-terminated case with the corresponding local moment shown in  $()$ .

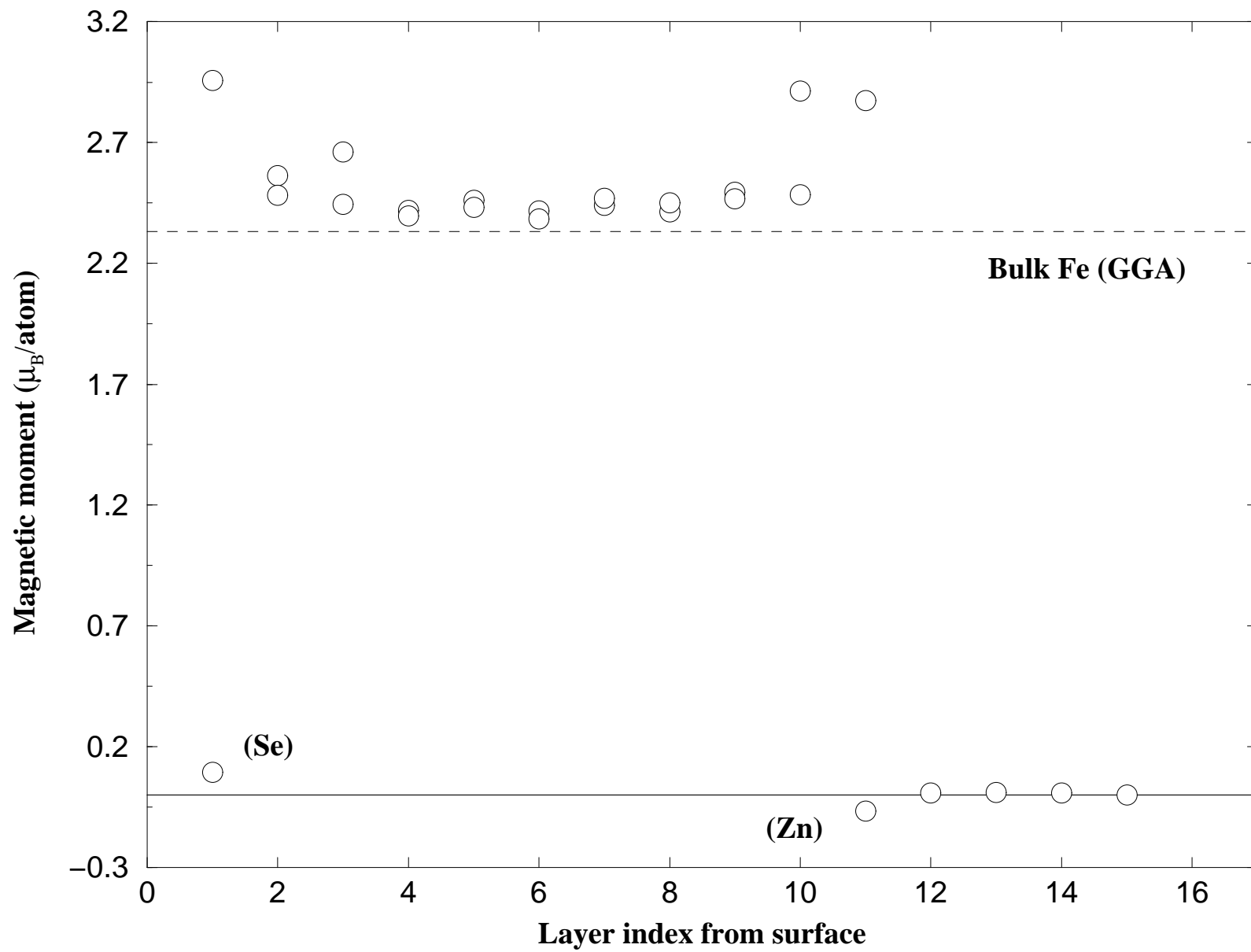
Thickness of Fe layers	$\text{Fe}_S\text{-Se}_S$ distance ( $\text{\AA}$ )	$\text{Fe}_I\text{-Zn}_I$ distance ( $\text{\AA}$ )	$\text{Fe}_I$ moment ( $\mu_B$ )
0.5 ML	2.52 (2.49) <sup>†</sup>	2.96 (2.37) <sup>*</sup>	2.84 (2.93)
1.5 ML	2.48	2.78	2.89
2.0 ML	2.74	2.77	2.74
10.0 ML	2.81	2.87	2.88



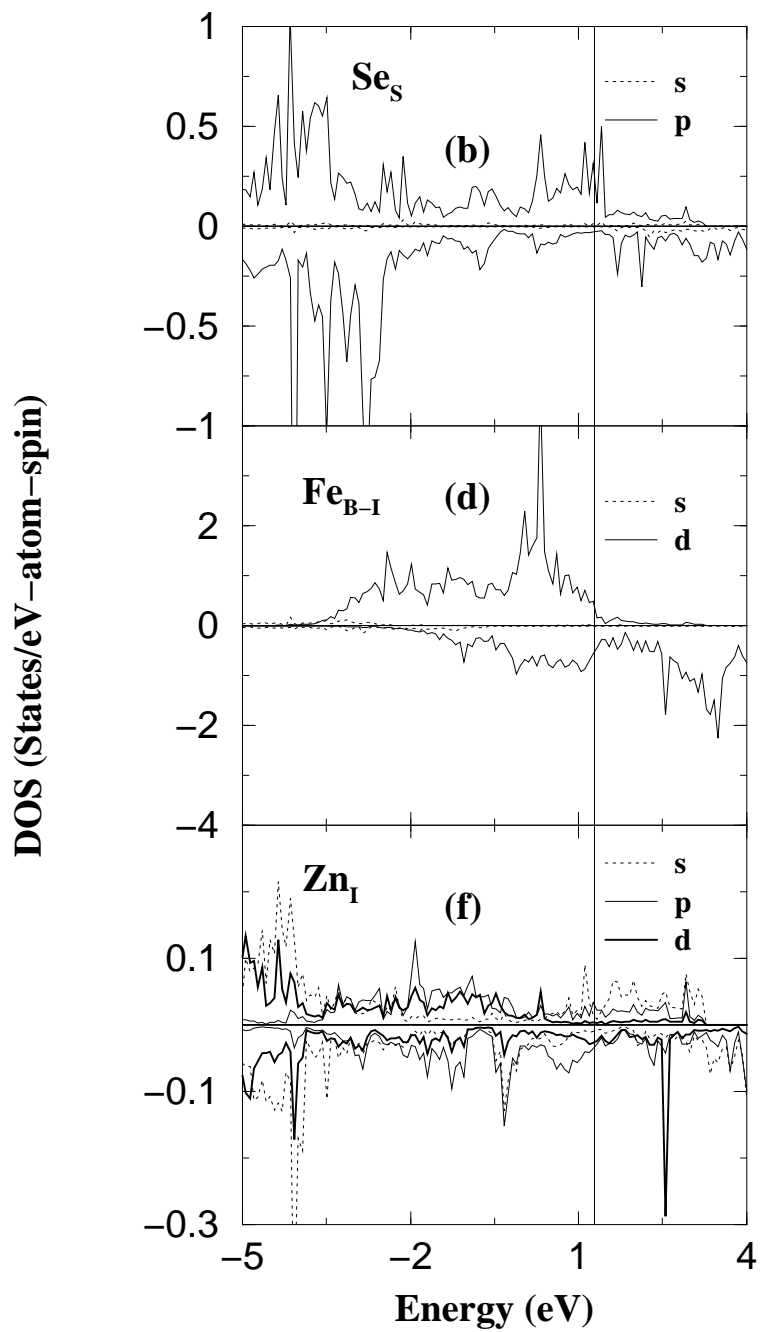
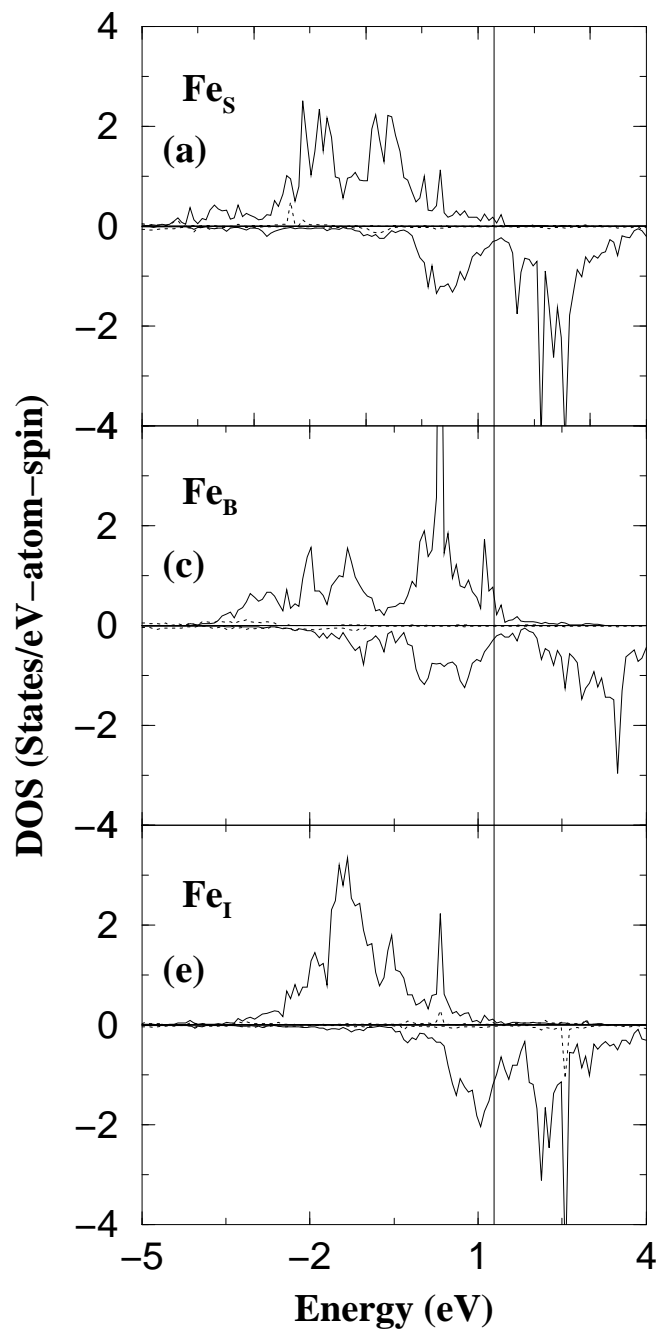


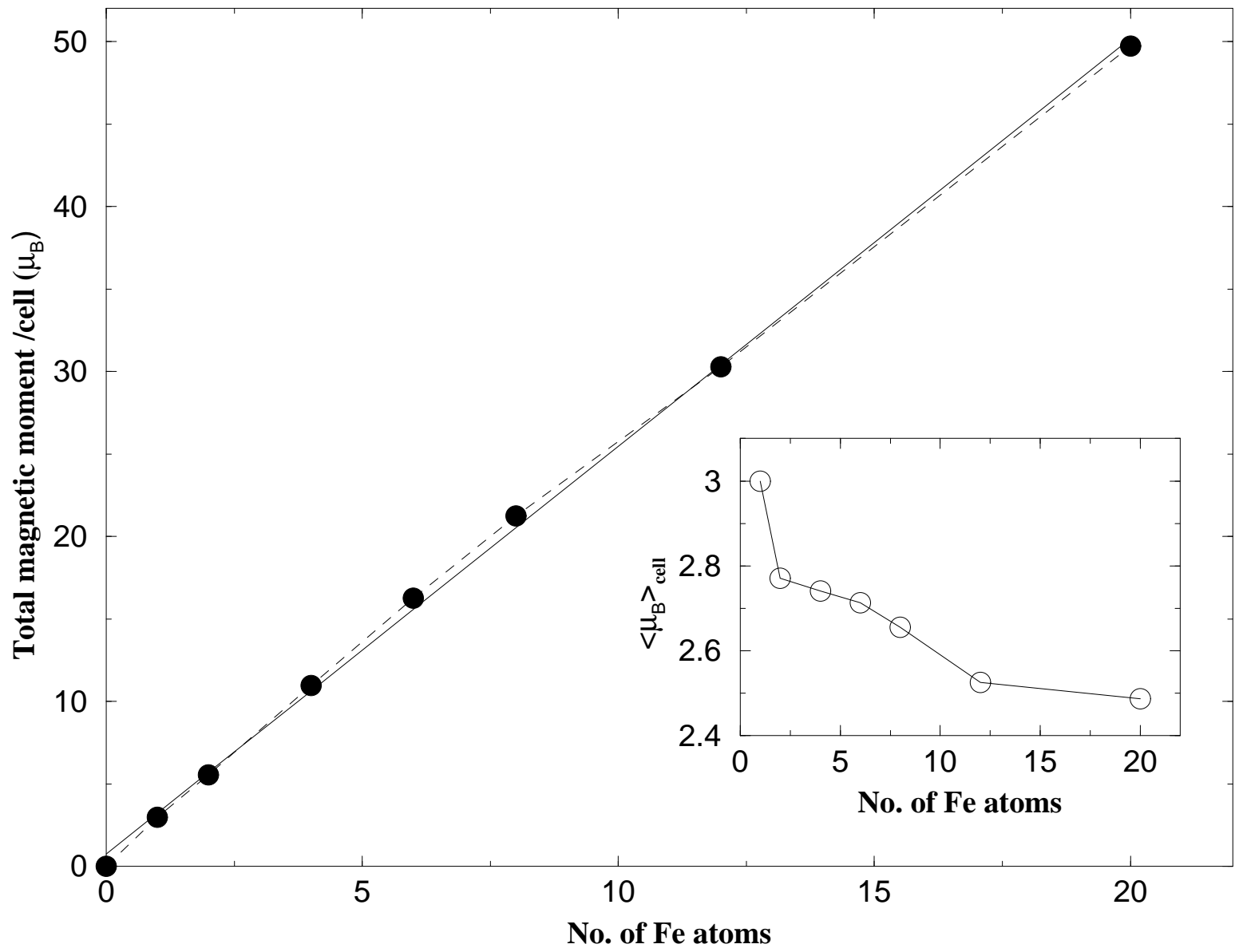


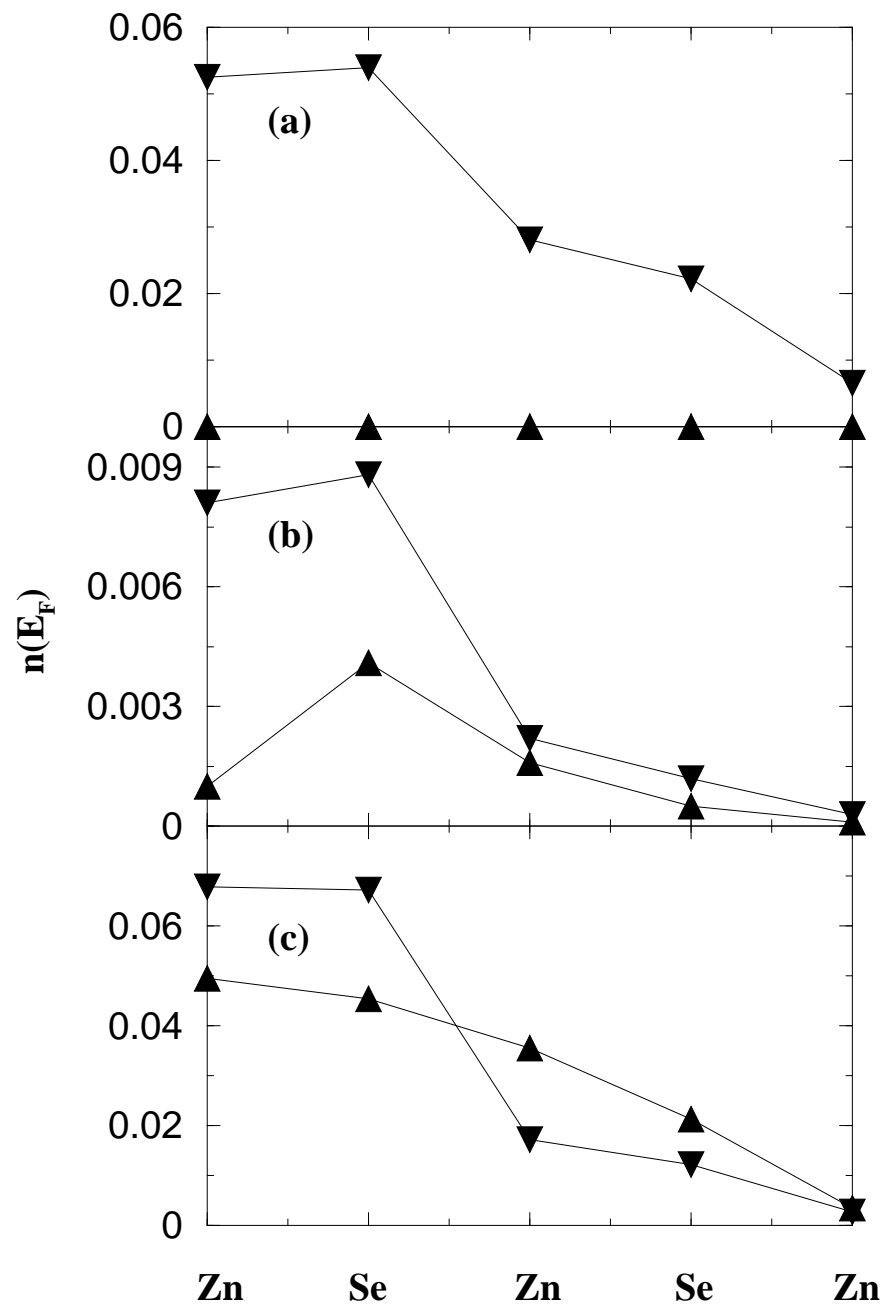










**Se term.****Zn term.**